ACS Biomaterials SCIENCE & ENGINEERING
Cite This: ACS Biomater. Sci. Eng. 2019, 5, 6274−6280
Article
pubs.acs.org/journal/abseba

Sandwich-type Surface Stress Biosensor Based on Self-Assembled Gold Nanoparticles in PDMS Film for BSA Detection

Dong Zhao,[†] Qiang Zhang,[†] Yixia Zhang,[†,‡] Yan Liu,[†] Zhen Pei,[†] Zhongyun Yuan,[†] and Shengbo Sang*[,†]

[†]MicroNano System Research Center, Key Lab of Advanced Transducers and Intelligent Control System of the Ministry of Education & College of Information and Computer and [‡]Department of Biomedical Engineering, Shanxi Key Laboratory of Material Strength & Structural Impact, College of Mechanics, Taiyuan University of Technology, Taiyuan 030024, China

Supporting Information

ABSTRACT: Poly(dimethylsiloxane) (PDMS) films composed of gold nanomaterials have drawn increasing interest for their application in biosensors. However, gold and PDMS exhibit poor compatibility, limiting their sensitivity in biosensing. Herein, we reported a surface stress biosensor based on a gold nanoparticle−PDMS (AuNP−PDMS) composite film to detect bovine serum albumin (BSA). The AuNP−PDMS film was fabricated by in situ reduction of PDMS and further reduction of glucose. The compatibility between gold and PDMS was improved via a two-step reduction of AuNPs. The surface stress biosensor can specifically detect BSA molecules within the 0−50 μg/mL concentration range using the direct assay and the sandwich assay. The sandwich assay amplified the surface stress and reduced the limit of detection to 0.035 μg/mL, which is lower than that achieved by the direct assay. The sandwich-type biosensor also exhibits stability, repeatability, and specificity. This study is expected to drive the development of new methods for biomolecule detection.

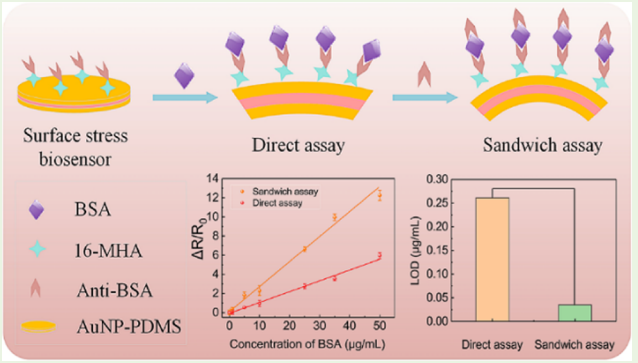

KEYWORDS: *self-assembly AuNPs, surface stress biosensor, sandwich assay, BSA detection*

1. INTRODUCTION

Nephropathy is a global health problem that poses a considerable threat to human life. Microalbuminuria is the presence of human serum albumin (HSA) at concentrations exceeding 30 μg/mL and is an early signal of nephropathy.[1,2] The severity of glomerular lesions can be inferred from the HSA concentration in urine. Therefore, detection of HSA in urine is highly significant.[3] Owing to its structural homology with HSA and affordability,[4−6] bovine serum albumin (BSA), instead of HSA, is frequently used in experimental tests.

Conventional approaches to detecting BSA include radioimmunoassay and enzyme-linked immunosorbent assay.[7] The probe method also has been used to establish a BSA-sensing system;[8] however, the sensitivity and detection range still need to be improved. Luminescence labeling and fluorescence labeling have been employed in BSA detection and shown a low limit of detection (LOD).[9,10] Nevertheless, these methods involve expensive reagents and complex preparation, restricting the application of these techniques.[11,12] Therefore, label-free, low-consumption, and high-consistency materials and methods need to be developed for BSA determination.

Gold nanoparticle−poly(dimethylsiloxane) (AuNP−PDMS) composite plays a critical role in sensitive membrane materials. The composite, which exhibits conductivity, high-strain performance, chemical stability, and biocompatibility,[13−17] can be applied to biosensors. Owing to their sensitivity to surface stress, the AuNPs−PDMS can be used in the design of a label−free biomolecule detection system.[18,19] Extensive studies have been conducted on the preparation of AuNP−PDMS composite. The AuNP−PDMS composite freestanding films have been fabricated by immersing cured PDMS sheets into an aqueous chloroauric acid ($HAuCl_4$) solution; however, the scarcity and uneven distribution of AuNPs led to the poor conductivity of PDMS.[20] In another report, the AuNPs were evaporated or sputtered on the surface of PDMS to prepare AuNP−PDMS composite.[21] However, these techniques entailed high costs and were complex to operate. Currently, the AuNP−PDMS composite is still widely used in biosensor investigation due to its nontoxicity and ease of functionalization.[22−24] However, the poor compatibility between gold and PDMS causes gold to easily fall off the surface of PDMS and affect the performance in high-precision biosensing. Moreover, few concerns were raised on the self-assembly of gold nanostructure in PDMS to fabricate the AuNP−PDMS composite and improve their compatibility.

Received: July 16, 2019
Accepted: October 14, 2019
Published: October 14, 2019

Downloaded via UNIV OF GLASGOW on July 18, 2020 at 10:56:12 (UTC).
See https://pubs.acs.org/sharingguidelines for options on how to legitimately share published articles.

© 2019 American Chemical Society

DOI: 10.1021/acsbiomaterials.9b01073
ACS Biomater. Sci. Eng. 2019, 5, 6274−6280

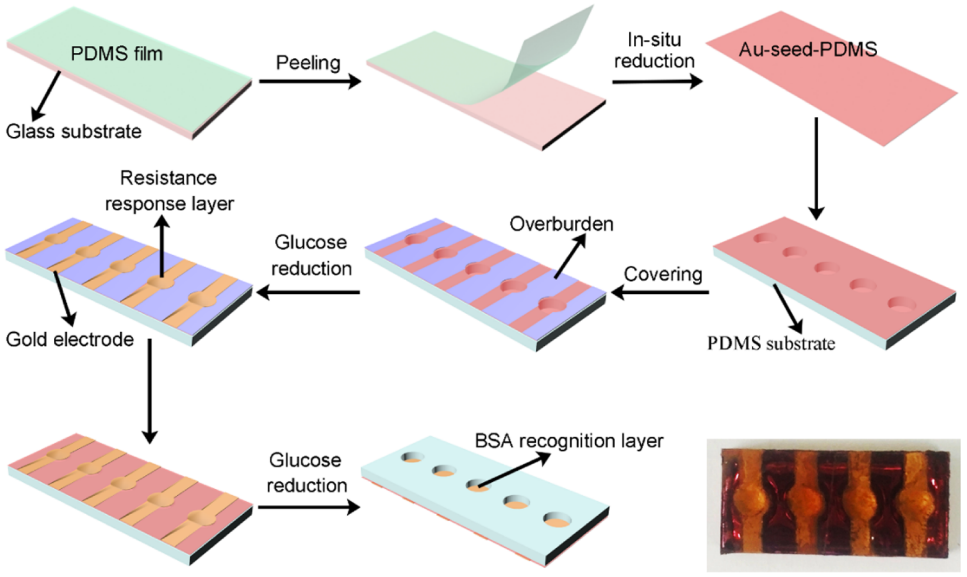

Figure 1. Fabrication procedure of the biosensor.

In the present study, we demonstrated a surface stress biosensor based on an AuNP−PDMS composite film for BSA detection. The AuNPs were self-assembled on PDMS by a two-step reduction method. BSA was detected using a surface stress biosensor via direct assay and sandwich assay. The biosensors were characterized by ultraviolet−visible (UV−vis) absorption spectroscopy, fluorescence microscopy, and scanning electron microscopy (SEM). Furthermore, the surface stress sensing principle of the biosensor was investigated as well. Overall, the developed sandwich-type surface stress biosensor is of significance for the diagnosis of nephropathy.

2. MATERIALS AND METHODS

2.1. Materials. BSA, BSA antibody (anti-BSA), phosphate-buffered saline (PBS, pH = 7.4), 1-ethyl-3-carbodiimide (EDC), *N*-hydroxysulfosuccinimide (NHS), 16-mercaptohexadecanoic acid (16-MHA), peptide, protease, collagen, and hemoglobin were provided by Sigma-Aldrich (Saint Louis, MO) and used without further purification. PDMS (Sylgard 184 silicone elastomer kit) was purchased from Dow Corning (Midland, MI). Chloroauric acid tetrahydrate ($HAuCl_4{\cdot}4H_2O$, Au ≥ 47.8%) was obtained from Sinopharm Chemical Reagent Co., Ltd. (Shanghai, CHN). Glucose ($C_6H_{12}O_6{\cdot}H_2O$, ≥99.5%) was purchased from Hengxing Chemical Reagents (Tianjin, CHN). Potassium bicarbonate ($KHCO_3$, ≥99.5%) was purchased from Fuchen Chemical Regents (Tianjin, CHN).

2.2. Preparation of Biosensor Based on Surface Stress. A PDMS prepolymer and a curing agent with a 10:1 weight ratio were mixed and placed at −20 °C for 2 h to remove bubbles. The PDMS was spin-coated onto glass substrates at 3000 rpm for 1 min using a spin coater (SPIN-1200D, Midas, Korea), forming 18 μm films. The PDMS films were further cured at 70 °C for 4 h, followed by peeling off the glass substrate. Subsequently, 5 mm thick PDMS substrates were fabricated and designed with holes measuring 4 mm in diameter. These holes allowed the film to deform under surface stress.

During in situ reduction, the PDMS films were incubated in a 0.01 g/mL $HAuCl_4$ alcohol solution for 24 h at room temperature. The PDMS films were then fixed on the PDMS substrate with uncured PDMS. During further reduction of glucose, the reducing solution was fabricated by mixing 0.01 g/mL $HAuCl_4$, 0.02 g/mL glucose, and 0.2 g/mL $KHCO_3$ in a volume ratio of 2:1:1. The surfaces of the PDMS film were partly covered with tapes (158080-ND, 3M). The PDMS films were treated twice with a reducing solution. In the first instance, the surfaces of the PDMS film remained in the reducing solution for 4 h at room temperature. The AuNPs, as electrodes and resistance response layers (RRLs) were prepared on the PDMS film surface. In the second instance, the reducing solution was added to the holes and kept for 4 h as well. The AuNPs, as the BSA recognition layers (BRLs), were formed on the other side of the PDMS film. The fabrication process and optical photography of the biosensor are shown in Figure 1.

2.3. Biosensors Characterization. UV−vis spectroscopy (UV-3100, Shimadzu, Japan) was conducted to measure the absorption spectra of AuNP−PDMS films. SEM (JSM-7400F, JEOL, Japan) was employed to observe the surface morphology of the AuNP−PDMS films. Fluorescence microscopy (DM3000, LEICA, Germany) was used to characterize fluorescently labeled BSA on the AuNP−PDMS films. Digital Multimeter (Keithley 2400, Tektronix) was purchased to test the electrical characteristics of the biosensor.

2.4. Biosensor Functionalization. The biosensors were thoroughly rinsed with acetone, isopropanol, ethanol, and deionized water for 3 min sequentially and then dried in nitrogen. The BRLs of the biosensor were treated with 5 mM 16-MHA for 6 h at room temperature. Then, the biosensors were cleaned with ethanol and deionized water to remove the 16-MHA residues. Equal volumes of 2 mM EDC and 5 mM NHS solutions were mixed directly, and the BRLs were activated for 2 h. The biosensors were ultimately immersed in 100 μg/mL anti-BSA for 2 h at room temperature and washed with deionized water and then dried under nitrogen.

2.5. BSA Detection. The BSA solutions at different concentrations were injected onto the BRL of the surface stress biosensor with a micropipette. Digital Multimeter probes were connected to the biosensor electrodes to evaluate the current−voltage characteristic curves. The diagram of the testing process is shown in Figure S1. The resistance change ($\Delta R/R_0$) of the RRL was calculated with eqs S1 and S2. Under similar experimental conditions, 10 parallel experiments were conducted to detect BSA at different concentrations. The standard deviation was obtained with eq S3. The relationship between $\Delta R/R_0$ and BSA concentration was fitted linearly. The mean-square error (MSE) and chi-square (χ^2) of the fitting curve were calculated using eqs S4 and S5, respectively.

3. RESULTS AND DISCUSSION

3.1. Self-Assembly of AuNPs in PDMS. The residual silicon hydrogen (Si−H) groups of PDMS reduced AuNPs in situ to prepare the AuNPs−PDMS composite film, which has been studied for decades. However, the inconsistency and insufficiency of AuNPs impede the study of electrical conductivity of composite films.[25,26] The electrical properties

DOI: 10.1021/acsbiomaterials.9b01073
ACS Biomater. Sci. Eng. 2019, 5, 6274−6280

of AuNPs on the PDMS surface are difficult to evaluate due to the lack of technologies to sustainably grow gold nanostructures. In this study, the in situ reduction of PDMS and further reduction of glucose provide a method to continuously perform self-assembly of AuNPs on the PDMS surface, as shown in Figure 2a. The AuNP−PDMS composite films were prepared, and high compatibility between AuNPs and PDMS was demonstrated by simple two-step self-assembly method. The schematic in Figure 2b shows the structure of the AuNP−PDMS composite film.

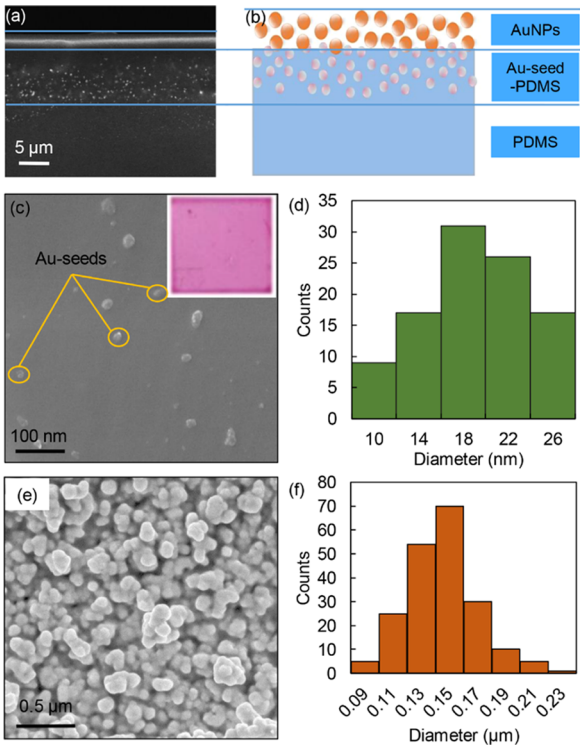

Figure 2. Characterization of the AuNP−PDMS. (a) SEM image and (b) schematic diagram of the AuNPs−PDMS composite film. (c) SEM image and optical image (inset) of PDMS with Au seeds (Au seed PDMS) after first step reduction. (d) Diameter distribution of Au seeds in the PDMS surface, as measured from the SEM images of samples of 200 particles using image processing. (e) SEM image of the distribution of gold nanostructures after glucose reduction. (f) Diameter distribution of AuNPs in PDMS surface after glucose reduction, as measured from the SEM images of samples of 200 particles using image processing.

During the in situ reduction of the PDMS, the Si−H groups pre-reduced $HAuCl_4$ to Au seeds. The Au seeds were embedded onto the PDMS surface for further AuNP formation and played an important role in improving the compatibility between gold and PDMS (Figure 2c). The diameter of the Au seed was 20.22 nm with a standard deviation of 1.29 nm (Figure 2d). Moreover, colorless PDMS turned purple-red, indicating the generation of Au seeds in PDMS via in situ reduction (inset in Figure 2d). In the glucose reduction, the AuNPs were further reduced and grew on the Au seed to form an even distribution of gold nanostructures (Figure 2e). The final AuNPs have an average diameter of 143 nm with a standard deviation of 24.9 nm (Figure 2f). The UV−vis absorption spectra confirmed the generation of AuNPs on the PDMS surface (Figure S2). The energy-dispersive spectrum (EDS) also reveals even the distribution of the Au seed and final AuNPs on the PDMS surface (Figure S3). The electrical properties of the biosensor exhibited sensitivity to micro-deformation (Figure S4).

3.2. Anti-BSA Modification of Biosensors. The process of anti-BSA modification is shown in Figure 3. A self-assembled layer (SAM) of 16-MHA for further antibody modification was formed on the BRL by chemical treatment. The NHS/EDC solution enabled the activation of carboxyl groups (−COOH) on SAM. The anti-BSA was modified on the BRL by forming a covalent bond with activated −COOH groups. The BSA could be specifically recognized and captured by the anti-BSA-modified BRL of surface stress biosensor.

3.3. Response Principle Analysis of the Biosensor. The as-prepared biosensor operates based on the surface stress from antigen−antibody binding. Thus, signals captured by the biosensor need to be induced by surface stress during biomolecular detection. As a proof of demonstration, we designed the control experiments and detected the BSA (20 μg/mL) and PBS with antimodified and antifree-surface stress biosensors, respectively. The dynamic responses of the biosensors are shown in Figure 4a. In the initial stages of the tests, the gravity of the buffer caused the concave deformation of the biosensor, generating a first resistance change equal to −3.51 on the RRL (Figure 4a). No surface stress was generated on the BRL; thus, the $\Delta R/R_{01}$ on the RRL of the antifree biosensor with BSA and antimodified biosensor with PBS remained at −3.51 within 0−20 min. However, the $\Delta R/R_{02}$ on the RRL of the antimodified biosensors gradually increased from −3.51 to 2.12 during the BSA detection (Figure 4a). The upward surface stress increased gradually on the BRL and eventually exceeded the gravity of the buffer. The biosensor also gradually deformed from concave to convex. After the resistance of each RRL was stabilized, the buffers were removed from the BRL, and the biosensor resistance of each was measured again. The $\Delta R/R_{02}$ of the antimodified biosensor with BSA only increased from 2.12 to 2.28 due to the presence of surface stress on the BRL, as shown in Figure 4b. However, the $\Delta R/R_{01}$ of the other two biosensors was restored to the initial value (Figure 4b). Therefore, surface stress is considered as the ultimate cause of biosensor

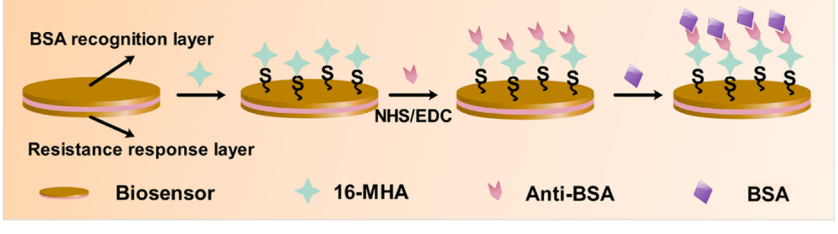

Figure 3. Schematic diagram of the modification procedure of the biosensor.

DOI: 10.1021/acsbiomaterials.9b01073
ACS Biomater. Sci. Eng. 2019, 5, 6274−6280

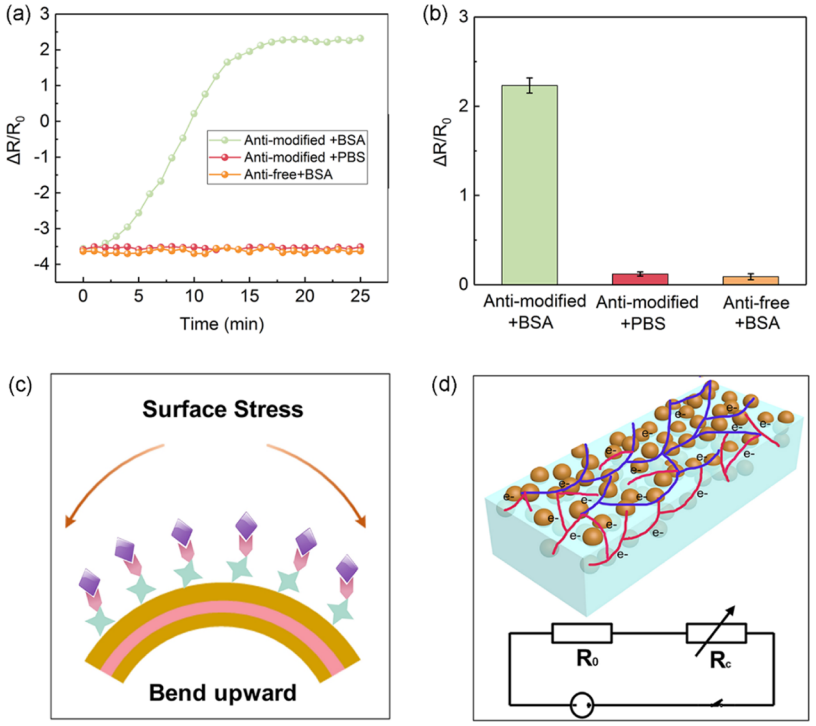

Figure 4. Response principle of surface stress biosensor. (a) Dynamic response of the antimodified and antifree surface stress biosensor to 10 μL of BSA (20 μg/mL) and 10 μL of PBS. Negative sign indicates resistance change caused by concave deformation of thin film. (b) Resistance change of antimodified and antifree biosensor after removing BSA and PBS without binding. (c) Schematic diagram of response mechanism of surface stress biosensor. (d) Resistance change mechanism diagram of surface stress biosensor.

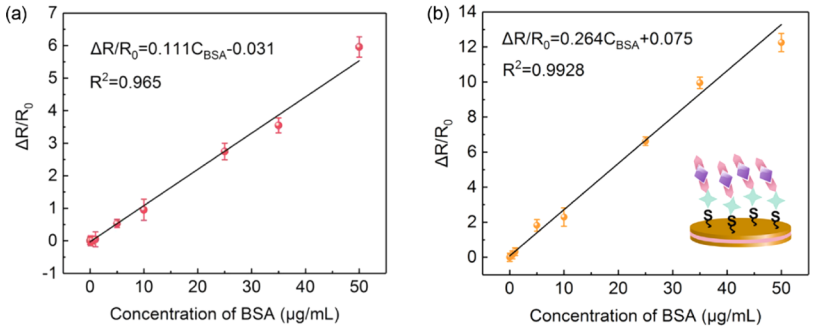

Figure 5. Response curves and standard deviation of BSA detection with different assays: (a) direct assay and (b) sandwich assay. The curves correspond to the resistance change of surface stress biosensor to the BSA concentrations ranging from 0 to 50 μg/mL.

resistance change. In the subsequent experiments, the final resistance changes of the biosensor were obtained after removing the buffer. The mechanism of resistance change is examined as well. The surface stress on the BRL enables the biosensor to convexly deform, resulting in the elongation of distance between AuNPs on the RRL[20,21,27] (Figure 4c,d). Therefore, the decrease in the conductive path led to an increase in the resistance of the RRL (Figure 4d). When the surface stress was generated, the R_C in the equivalent circuit increased and the electrode resistance R_0 remained unchanged (Figure 4d).

3.4. Direct Assay and Sandwich Assay of BSA. The analytical performance of the direct assay was studied using 10 μL of BSA solutions at various concentrations in the anti-BSA-modified BRL of the surface stress biosensor. The BSA molecules could be specifically recognized by the BRL (Figure S5). The response curve of biosensor to the BSA is depicted in Figure 5a. The resistance change of the RRL exhibited a linear relationship with the BSA concentration from 0 to 50 μg/mL. The linear equation is given by $\Delta R/R_0 = 0.111C_{BSA} - 0.031$ ($R^2 = 0.965$, MSE = 0.44, $\chi^2 = 1.25 \times 10^{-5}$). The 10 parallel tests of BSA exhibited a high-performance repeatability. The LOD was calculated to be 0.261 μg/mL with the formula LOD = $3\sigma/S$, where σ is the standard deviation of the 10 blank measurements and S is the slope of the linear curve.[28]

To further investigate the sandwich assay of the surface stress biosensor, the 50 μg/mL anti-BSA was selected as the secondary antibody. The BSA solutions were first kept for 20 min on the anti-BSA-modified BRL of the biosensor. Subsequently, 50 μg/mL anti-BSA was dripped onto the BRL of the biosensor and kept for 20 min and then removed from the BRL. An anti-BSA/BSA/anti-BSA interaction occurred on the BRL of the biosensor. The second specific binding of BSA to anti-BSA amplified the surface stress on the BRL, causing a larger convex deformation on the biosensor. The resistance change of the RRL increased more significantly

DOI: 10.1021/acsbiomaterials.9b01073
ACS Biomater. Sci. Eng. 2019, 5, 6274−6280

Table 1. Comparison of Analytical Methods Reported for BSA Detection

material	method	detection range	LOD	refs
diketopyrrolopyrrole and anthracenone conjugates	probes	0.33−6.65 mg/mL	0.33 mg/mL	8
ruthenium(II) polypyridine complexes	luminescence detection	0−66.5 μg/mL	19.95 μg/mL	9
chemically converted graphene (ccg)	fluorescence detection	3.3−532 μg/mL	3.3 μg/mL	10
nitrocellulose membrane	electrochemistry	5−100 μg/mL	1.78 μg/mL	29
AuNPs−PDMS membrane	surface stress & direct assay	0−50 μg/mL	0.26 μg/mL	this work
	surface stress & sandwich assay	0−50 μg/mL	0.035 μg/mL	

in the sandwich assay than in the direct assay, as shown in Figure 5a,b. The linear equation is represented by $\Delta R/R_0 = 0.264C_{BSA} + 0.075$ ($R^2 = 0.9928$, MSE = 0.23, $\chi^2 = 3.16 \times 10^{-6}$). The LOD of the sandwich-type biosensor was 0.035 μg/mL, which was lower than that of the direct assay. The biosensors exhibited good repeatability, as indicated by 10 sandwich assays of BSA.

Table 1 compares the performances of the surface stress biosensor with those of several other reported methods of BSA detection. The as-prepared surface stress biosensor has a lower LOD than those of other biosensors.[8−10] Specifically, the LOD of the as-prepared sandwich-type biosensor was improved. The as-prepared biosensor demonstrated its advantage over the probe method with respect to the detection range;[8,9] however, luminescence detection, fluorescence detection, and electrochemistry were superior.[10,29] Furthermore, the AuNP−PDMS membrane involved a simple preparation method and exhibited a low consumption. Therefore, the as-prepared sandwich-type surface stress biosensor shows a potential for applications in the BSA detection.

3.5. Stability of the Surface Stress Biosensor. The stability of the surface stress biosensor was studied by tracking its response to 20 μg/mL BSA with a sandwich assay at the same intervals of time. The biosensors were modified using the anti-BSA under similar conditions and stored at 4 °C. For every single detection cycle, the BRL of the biosensor was combined with the BSA solution and 50 μg/mL anti-BSA for 20 min, respectively, and then the buffer was removed. The response of the biosensor after the daily time span is shown in Figure 6. The resistance changes of the RRL were nearly constant with a relative standard deviation of 2.1%, indicating the excellent stability of the biosensor for BSA detection.

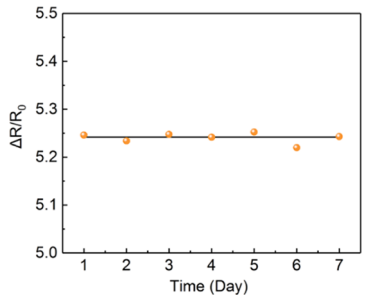

Figure 6. Stability measurement of 20 μg/mL BSA on the surface stress biosensor.

3.6. Specificity of the Surface Stress Biosensor. To study the specificity of the surface stress biosensor, BSA, peptide, protease, collagen, and hemoglobin, each at a concentration of 20 μg/mL, were detected with a sandwich assay. The resistance changes of biosensor are shown in Figure 7. The biosensor with BSA results in a considerable variation in resistance, indicating the high specificity for BSA detection. A mixtures of BSA with other biomolecules were also analyzed using the biosensor, revealing the high-performance selectivity of the biosensor (Figure S6). Hence, the surface stress biosensors have potential for application in urinalysis.

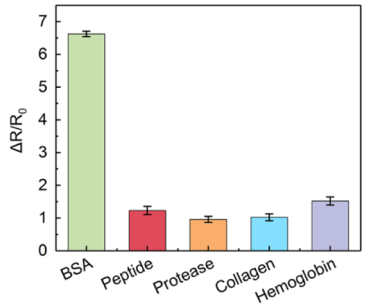

Figure 7. Resistance changes of surface stress biosensor caused by different biomolecules.

4. CONCLUSIONS

In summary, a surface stress biosensor based on an AuNP−PDMS film was fabricated for sensitive BSA detection. The compatibility between gold and PDMS was improved by in situ reduction of PDMS and further reduction of glucose. Surface stresses from the specific recognition of BSA and anti-BSA was captured by the biosensor. The surface stress biosensor successfully detected BSA at wide concentrations ranging from 0 to 50 μg/mL with direct assay and sandwich assay. The anti-BSA, as the secondary antibody, effectively reduced the LOD of the biosensor to 0.035 μg/mL, which is an order of magnitude lower than that achieved with direct assay. In addition, the biosensor exhibits good specificity and stability for BSA detection. The study not only provides a method for BSA detection but also shows its application potential in biomolecular detection

■ ASSOCIATED CONTENT

Supporting Information

The Supporting Information is available free of charge on the ACS Publications website at DOI: 10.1021/acsbiomaterials.9b01073.

Test process diagram of BSA; UV−vis absorption spectrum of asymmetric sandwich structure film; energy-dispersive spectrum (EDS) of AuNPs−PDMS film; electrical properties of the biosensor; fluorescence images of biosensors surface with BSA at different concentrations; selectivity of biosensor; and methods of calculating the resistance change, standard deviation, MSE, and χ^2 of linear-fitting curves (PDF)

DOI: 10.1021/acsbiomaterials.9b01073
ACS Biomater. Sci. Eng. 2019, 5, 6274−6280

AUTHOR INFORMATION

Corresponding Author

*E-mail: sunboa-sang@tyut.edu.cn.

ORCID

Shengbo Sang: 0000-0003-3011-7632

Author Contributions

D.Z. and Q.Z. contributed equally to this work. The manuscript was written through contributions of all authors. All authors have given approval to the final version of the manuscript.

Notes

The authors declare no competing financial interest.

ACKNOWLEDGMENTS

The authors are grateful for the support by the National Natural Science Foundation of China (Nos. 51622507, 61703298, 61474079, and 51705354), Basic Research Program of Shanxi for Youths (Nos. 201701D221110 and 2015021092), and the Graduate Student Education Innovation Project of Shanxi (the study of surface stress biosensor based on tunneling conductive AuNP−PDMS composite film).

ABBREVIATIONS

AuNP−PDMS,gold nanoparticle−PDMS; BSA,bovine serum albumin; HAS,human serum albumin; anti-BSA,BSA antibody; PBS,phosphate-buffered saline; EDC,1-ethyl-3-carbodiimide; NHS,*N*-hydroxysulfosuccinimide; 16-MHA,16-mercaptohexadecanoic acid; RRL,resistance response layer; BRL,BSA recognition layer; UV−vis,ultraviolet−visible; $\Delta R/R_0$,resistance change; MSE,mean-square error; χ^2,chi-square; EDS,energy-dispersive spectrum; SAM,self-assembled layer

REFERENCES

(1) Fan, J.; Sun, W.; Wang, Z.; Peng, X.; Li, Y.; Cao, J. A fluorescent probe for site I binding and sensitive discrimination of HSA from BSA. *Chem. Commun.* **2014**, *50*, 9573−9576.

(2) Hopp, I.; MacGregor, M. N.; Doherty, K.; Visalakshan, R. M.; Vasilev, K.; Williams, R. L.; Murray, P. Plasma Polymer Coatings To Direct the Differentiation of Mouse Kidney-Derived Stem Cells into Podocyte and Proximal Tubule-like Cells. *ACS Biomater. Sci. Eng.* **2019**, *5*, 2834−2845.

(3) Rajasekhar, K.; Achar, C. J.; Govindaraju, T. A red-NIR emissive probe for the selective detection of albumin in urine samples and live cells. *Org. Biomol. Chem.* **2017**, *15*, 1584−1588.

(4) Mariee, A. D.; Al-Shabanah, O. Protective ability and binding affinity of captopril towards serum albumin in an in vitro glycation model of diabetes mellitus. *J. Pharm. Biomed. Anal.* **2006**, *41*, 571−575.

(5) Yokoyama, S.; Takeda, T.; Abe, M. Preparation of ganglioside GM3 liposomes and their membrane properties. *Colloids Surf., B* **2003**, *27*, 181−187.

(6) Memon, A. H.; Ding, R.; Yuan, Q.; Liang, H.; Wei, Y. Coordination of GMP ligand with Cu to enhance the multiple enzymes stability and substrate specificity by co-immobilization process. *Biochem. Eng. J.* **2018**, *136*, 102−108.

(7) Lin, T.-Y.; Hu, C.-H.; Chou, T.-C. Determination of albumin concentration by MIP-QCM sensor. *Biosens. Bioelectron.* **2004**, *20*, 75−81.

(8) Wang, L.; Yang, L.; Cao, D. Probes based on diketopyrrolopyrrole and anthracenone conjugates with aggregation-induced emission characteristics for pH and BSA sensing. *Sens. Actuators, B* **2015**, *221*, 155−166.

(9) Babu, E.; Muthu Mareeswaran, P.; Singaravadivel, S.; Bhuvaneswari, J.; Rajagopal, S. A selective, long-lived deep-red emissive ruthenium(II) polypyridine complexes for the detection of BSA. *Spectrochim. Acta, Part A* **2014**, *130*, 553−560.

(10) Li, H.; Liu, F.; Han, J.; Cai, M.; Sun, S.; Fan, J.; Song, F.; Peng, X. Interaction of Cy3 dye with CCG and its application for BSA detection. *J. Mater. Chem. B* **2013**, *1*, 693−697.

(11) Tian, T.; Li, J.; Song, Y.; Zhou, L.; Zhu, Z.; Yang, C. J. Distance-based microfluidic quantitative detection methods for point-of-care testing. *Lab Chip* **2016**, *16*, 1139−1151.

(12) Liu, D.; Li, X.; Zhou, J.; Liu, S.; Tian, T.; Song, Y.; Zhu, Z.; Zhou, L.; Ji, T.; Yang, C. A fully integrated distance readout ELISA-Chip for point-of-care testing with sample-in-answer-out capability. *Biosens. Bioelectron.* **2017**, *96*, 332−338.

(13) Zimmermann, J.; Artus, G. R. J.; Seeger, S. Long term studies on the chemical stability of a superhydrophobic silicone nanofilament coating. *Appl. Surf. Sci.* **2007**, *253*, 5972−5979.

(14) Wang, D.; Ba, D.; Hao, Z.; Li, Y.; Sun, F.; Liu, K.; Du, G.; Mei, Q. A novel approach for PDMS thin films production towards application as substrate for flexible biosensors. *Mater. Lett.* **2018**, *221*, 228−231.

(15) Cheng, M. Y.; Tsao, C. M.; Lai, Y. Z.; Yang, Y. J. The development of a highly twistable tactile sensing array with stretchable helical electrodes. *Sens. Actuators, A* **2011**, *166*, 226−233.

(16) Spencer, A. R.; Primbetova, A.; Koppes, A. N.; Koppes, R. A.; Fenniri, H.; Annabi, N. Electroconductive Gelatin Methacryloyl-PEDOT:PSS Composite Hydrogels: Design, Synthesis, and Properties. *ACS Biomater. Sci. Eng.* **2018**, *4*, 1558−1567.

(17) Abraham, A. A.; Means, A. K.; Clubb, F. J.; Fei, R.; Locke, A. K.; Gacasan, E. G.; Coté, G. L.; Grunlan, M. A. Foreign Body Reaction to a Subcutaneously Implanted Self-Cleaning, Thermoresponsive Hydrogel Membrane for Glucose Biosensors. *ACS Biomater. Sci. Eng.* **2018**, *4*, 4104−4111.

(18) Butt, H. A Sensitive Method to Measure Changes in the Surface Stress of Solids. *J. Colloid Interface Sci.* **1996**, *180*, 251−260.

(19) Sang, S.; Zhao, Y.; Zhang, W.; Li, P.; Hu, J.; Li, G. Surface stress-based biosensors. *Biosens. Bioelectron.* **2014**, *51*, 124−135.

(20) Sang, S.; Witte, H. A novel PDMS micro membrane biosensor based on the analysis of surface stress. *Biosens. Bioelectron.* **2010**, *25*, 2420−2424.

(21) Sang, S.; Witte, H. Fabrication of a surface stress-based PDMS micro-membrane biosensor. *Microsyst. Technol.* **2010**, *16*, 1001−1008.

(22) Roper, D. K.; Bern, K. R., Jr; Dunklin, J. R.; Chambers, C.; Bejugam, V.; Forcherio, G. T.; Lanier, M. Effects of geometry and composition of soft polymer films embedded with nanoparticles on rates for optothermal heat dissipation. *Nanoscale* **2018**, *10*, 11531−11543.

(23) Zhao, D.; Liu, Y.; Zhang, Q.; Zhang, Y.; Zhang, W.; Duan, Q.; Yuan, Z.; Zhang, R.; Sang, S. Surface stress-based biosensor with stable conductive AuNPs network for biomolecules detection. *Appl. Surf. Sci.* **2019**, *491*, 443−450.

(24) Cha, W.; Kim, H.; Lee, S.; Kim, J. Size-controllable and stable organometallic halide perovskite quantum dots/polymer films. *J. Mater. Chem. C* **2017**, *5*, 6667−6671.

(25) Scarano, S.; Berlangieri, C.; Carretti, E.; Dei, L.; Minunni, M. Tunable growth of gold nanostructures at a PDMS surface to obtain plasmon rulers with enhanced optical features. *Microchim. Acta* **2017**, *184*, 3093−3102.

(26) Joseph Fortenbaugh, R.; Lear, B. J. On-demand curing of polydimethylsiloxane (PDMS) using the photothermal effect of gold nanoparticles. *Nanoscale* **2017**, *9*, 8555−8559.

(27) Jian, A.; Tang, X.; Feng, Q.; Duan, Q.; Ji, J.; Ma, Z.; Zhang, W.; Sang, S. A PDMS surface stress biosensor with optimized micro-membrane: Fabrication and application. *Sens. Actuators, B* **2017**, *242*, 969−976.

(28) Guo, X.; Sang, S.; Guo, J.; Jian, A.; Duan, Q.; Ji, J.; Zhang, Q.; Zhang, W. A magnetoelastic biosensor based on E2 glycoprotein for wireless detection of classical swine fever virus E2 antibody. *Sci. Rep.* **2017**, *7*, No. 15626.

(29) Zhang, D.; Lu, Y.; Zhang, Q.; Liu, L.; Li, S.; Yao, Y.; Jiang, J.; Liu, G. L.; Liu, Q. Protein detecting with smartphone-controlled

DOI: 10.1021/acsbiomaterials.9b01073
ACS Biomater. Sci. Eng. 2019, 5, 6274−6280

electrochemical impedance spectroscopy for point-of-care applications. *Sens. Actuators, B* **2016**, *222*, 994−1002.

DOI: 10.1021/acsbiomaterials.9b01073
ACS Biomater. Sci. Eng. 2019, 5, 6274−6280